FERMILAB-PUB-74-137-E
CERN/D.Ph.II/PHYS 74-26
28.6.1974

THE REACTION $\pi^- p \to \pi^- \pi^+ \pi^- p$ AT 100 GeV/c

E.L. Berger*, V.T. Cocconi, M.J. Counihan**, S. Humble***, G. Kellner, A. Kotanski+, D. Kuhn++, S.B. Ljung+++, D.R.O. Morrison, P. Schmido, R. Stroynowski, F.A. Triantis and H. Wahl.

CERN, Geneva

ABSTRACT

The reaction $\pi^- p \to \pi^- \pi^+ \pi^- p$ at 100 GeV/c has been analysed in terms of effective mass and rapidity variables. It is found to be dominated by two well-separated processes, i.e. the diffractive dissociation of the pion and that of the proton. The diffractive nature of these processes is confirmed by the weak energy dependence of the cross section for the reaction, which falls like $p_{LAB}^{-0.25}$ between 5 and 200 GeV/c. A small class of events is found having the properties expected for "double Pomeron exchange", $\pi^- p \to \pi^- (\pi^- \pi^+) p$. The cross section for such events is estimated to be 40 ± 20μb.

* Visiting Scientist from Argonne National Laboratory.

** CERN Fellow from Imperial College, London.

*** Visiting Scientist from Daresbury Laboratory.

+ On leave from Jagellonian University, Cracow.

++ CERN Fellow from Physikalisches Institut der Universitat, Innsbruck.

+++ Visiting Scientist from Helsinki University.

o CERN Fellow from Institut für Hochenergiephysik, Vienna.

MJC/mk

The results presented here are based on a 50,000 photograph exposure of the 30" Argonne-MURA hydrogen bubble chamber at the Fermi National Accelerator Laboratory to 100 GeV/c negative pions. Measurements have been made of a sample of 1048 four-prong events whose vertex occurred in the upstream half of the chamber. Of these, 101 events gave four-constraint fits to the reaction

$$\pi^- p \rightarrow \pi^- \pi^+ \pi^- p \qquad (1)$$

We remark that these fits should properly be regarded as three-constraint fits since momentum conservation in the beam direction is effectively imposed on these evetns; this is because there is generally at least one fast forward track with a large measurement error on the magnitude of its momentum.

An examination of the detailed properties of the events fitting reaction (1) and of those which do not fit has satisfied us that there is little background in this sample. This is illustrated by fig. 1, which shows scatterplots of the squared missing mass of each event against the missing momentum component $p_\perp(y)$ in the direction perpendicular to both the beam direction and to the camera axis. This component of the missing transverse momentum is taken because the measurement precision is rather better than for the component parallel to the camera axis. The value of $\Delta p_\perp(y)$ is calculated from measured momenta the magnitudes of which have been adjusted so as to conserve momentum in the beam direction. Note that the squared missing mass measured for an event of the type (1) will be almost independent of any imprecision in the magnitude of the momentum of a fast particle. Fig. 1(a) shows the squared missing mass against $\Delta p_\perp(y)$ for the events which fitted reaction (1), and fig. 1(b) shows the same thing for candidate events which failed the fit. For the fits, the squared missing mass and $\Delta p_\perp(y)$ are both close to zero: the r.m.s. values are 0.297 GeV^2 and 0.151 GeV/c respectively. In contrast, the non-fitted events are widely spread in both these variables; in fact the great majority of them fall outside the boundaries of fig. 1(b).

The cross section obtained for reaction (1) at 100 GeV/c is 590 ± 70μb. This value, together with the 200 GeV/c cross section [1] are included in the plot of cross section againt lab. momentum shown in fig. 2. The straight line is a fit of the data above 5 GeV/c to the function

$$\sigma = K.\ p_{LAB}^{-n} \quad , \tag{2}$$

and gives a value 0.25 ± 0.03 for the exponent n.

The weak dependence of the cross section on lab. momentum indicates that this reaction is largely diffractive at these energies. This interpretation is consistent with fig. 3, which is a scatter plot of the effective mass $M(p\pi^+\pi^-)$ againt $M(\pi^-\pi^+\pi^-)$. (For $M(p\pi^+\pi^-)$, we take the combination including the slower of the two π^-'s, i.e. that with the smaller rapidity). There are two distinct accumulations of events, one with small $M(\pi^-\pi^+\pi^-)$ corresponding to the dissociation process

$$\pi^- p \rightarrow (\pi^-\pi^+\pi^-)p \tag{3}$$

and the other with small $(M(p\pi^+\pi^-)$ corresponding to

$$\pi^- p \rightarrow \pi^-(p\pi^+\pi^-). \tag{4}$$

It may be noted that there are a number of events in the lower left-hand corner of fig. 3 for which $M(\pi^-\pi^+\pi^-)$ and $M(p\pi^+\pi^-)$ are both fairly small, and which cannot be unambiguously assigned to either of the processes (3) and (4) above. These will be discussed in more detail below.

Fig. 4(a) and (b) are projections of fig. 3, i.e. the $(p\pi^+\pi^-)$ and $(\pi^-\pi^+\pi^-)$ mass spectra. The expected threshold enhancements are clearly visible, with essentially no background. It can be seen that the enhancements extend will above the masses of the resonance-like systems ($N^*(1470)$, $N^*(1710)$, $A_1(1100)$ and $A_3(1640)$) which are seen at lower energies to be diffractively produced in this reaction.

We have examined the problem of how to divide the events into classes corresponding to the reactions (3) and (4) above and

$$\pi^- p \to (\pi^- \pi^+)(\pi^- p) \tag{5}$$

$$\pi^- p \to (\pi^- \pi^-)(\pi^+ p) \tag{6}$$

and $$\pi^- p \to \pi^-(\pi^- \pi^+)p \tag{7}$$

which are illustrated in fig. 5(i) - (v) respectively. The first two of these are the single diffractive dissociation reactions (3) and (4); the last is the "double Pomeron exchange" reaction which may be expected [2] to contribute significantly to the cross section at this energy. In general the separation of events according to reaction mechanisms can be attempted by plotting the data in a two-dimensional form. On such method is the LPS analysis of Van Hove [3], where the Feynman variable x of the π^+ is plotted against that of the slower π^-. To help with problems such as the accumulation of events with $x(\pi^+) \sim x(\pi^-) \sim 0$ (where the phase space volume peaks sharply) there is some advantage in plotting rapidity, e.g. for the π^+ against y for the slow π^-, the rapidity being

$$y = \frac{1}{2} \ln \frac{E+p_{11}}{E-p_{11}} \tag{8}$$

for each particle, where E and p_{11} are the energy and longitudinal momentum respectively. Here we would like to suggest an extension of this method, which uses the concept of the "largest rapidity gap" as a means of separating different reaction mechanisms [4]. We take first the rapidity differences between the produced particles

$$y(p \to \pi^+) = y_{\pi+} - y_p \tag{9a}$$

$$y(p \to \pi_s^-) = y_{\pi_s^-} - y_p \tag{9b}$$

$$y(p \to \pi^-) = y_{\pi_f^-} - y_p \tag{9c}$$

where π_f^- is the faster of the two π^-'s, and π_s^- is the slower, i.e. $y_{\pi_f^-} > y_{\pi_s^-}$. Because of the leading particle effect $y(p \to \pi_f^-)$ is always large, close to the rapidity difference between the incident π^- and proton. It is found that on average $y(p \to \pi_f^-) = 5.7$, with an r.m.s. spread of only 0,73 about this value. We therefore define relative rapidities for the π^+ and the slower π^- by

$$\text{Rel.Rap. } (\pi^+) = y(p \to \pi^+) \;/\; y(p \to y_{\pi_f^-}) \tag{10a}$$

$$\text{Rel.Rap. } (\pi_s^-) = y(p \to \pi_s^-) \;/\; y(p \to y_{\pi_f^-}) \tag{10b}$$

Thus the "relative rapidity" of the π^+, say, is simply its rapidity (relative to the proton) normalised to that of the leading π^-.

The relative rapidities of the π^+ and π_s^- specify completely the configuration of the event, if transverse momenta can be neglected. For any specific values of these two variables, the absolute c.m. or lab. frame rapidities of all four produced particles are fixed by energy and momentum conservation. Fig. 6 shows the relative rapidity of the π_s^- against that of the π^+ for the events fitting reaction (1). Note that the relative rapidity of the π_s^- is always less than unity since the π_s^- is defined as being slower than the π_f^-. The cluster of events in the lower left hand corner corresponds to process (4), and that in the upper right hand corner corresponds to process (3), as indicated on the figure. This plot is particularly useful since the dotted lines shown divide the figure into the different regions which would correspond to the selection of different quasi-two-body reaction mechanisms according to the "largest rapidity gap" criterion. For example, the almost empty lower right hand region corresponds to the quasi-two-body process

$$\pi^- p \to (\pi^- \pi^+) \; (\pi^- p) \tag{11}$$

as defined by the requirements that a π^- and the π^+ are the fastest particles and that, when the four particles are ordered according to rapidity, the largest gap between an adjacent pair divides the particles into two systems as in (8) above.

Fig. 6 indicates that the diffractive processes (3) and (4) are well separated from each another and dominate the cross section, while the charge exchange processes (fig. 5(iii) and (iv)) are strongly suppressed. At the same time, there are some events in the centre of the plot near the boundary between the two heavily populated regions. They have the $\pi^+\pi_s^-$ pair close together in rapidity and about half way between the proton and the leading π_f^-. As was mentioned above, the plot of $M(\pi^-\pi^+\pi^-)$ against $M(p\pi^+\pi^-)$ shows a similar phenomenon.

These events may be associated with the double Pomeron exchange process of fig. 5(v). To estimate the corresponding cross section we may use any of a number of selection criteria which have been proposed [5] for the purpose. In particular, the selection based on rapidities

$$y_{\pi_f^-} - y_{\pi_s^-} > 2, \tag{12a}$$

$$y_{\pi_f^-} - y_{\pi^+} > 2, \tag{12b}$$

$$y_{\pi_s^-} - y_p > 2, \tag{12c}$$

and $$y_{\pi^+} - y_p > 2 \tag{12d}$$

corresponds to the selection of a square region in fig. 6 (at the centre of the plot, with side $\approx$ 0.3 units) containing 7 events. An alternative selection using the Feynman x variable (not illustrated) is

$$x_{\pi_f^-} > 0.9 \quad \text{and} \quad x_p < -0.9 \tag{13}$$

and this gives 8 events. The corresponding cross section for the events selected by such criteria is then 40 ± 20μb. As no background is assumed, this should be taken as an upper limit on double Pomeron exchange.

The cross sections found for diffractive proton dissociation and pion dissociation are not sensitive to the selection criteria used for these processes. Allowing for the variation of measurement efficiency for events of different configurations, we obtain 280 ± 40μb for proton dissociation and 240 ± 50μb for pion dissociation. However, we would like to point out that the pion dissociation cross section may be underestimated as a result of problems in the kinematic fitting of these events.

We are deeply indebted to the operating crews of the Fermi NAL accelerator and of the 30-inch bubble chamber. We would like to thank our scanning, measuring and computing staffs, and to acknowledge useful conversations with D.M. Chew.

REFERENCES

[1] D. Bogert el al., "$\pi^- p$ Interactions at 200 GeV/c", Fermi National Laboratory preprint NAL-Conf. 73/30-EXP (1973).

[2] R. Shankar, Nucl. Phys. B70 (1974) 168.

[3] W. Kittel, S. Ratti and L. Van Hove, Nucl. Phys. B30 (1971) 333
J.V. Beaupré et al., Nucl. Phys. B46 (1972) 1.

[4] G.F. Chew, "Weakly Recurrent Pomerons", Stony Brook Cenference 1973, A.I.P. Conference Prodeedings No. 15 (1973).

[5] D.M. Chew, "Search for Experimental Evidence on Exclusive Double-Pomeron Exchange", Lawrence Berkely Laboratory, preprint LBL-3009 (1974) and references therein.

FIGURE CAPTIONS

Fig. 1 Scatter plots of the squared missing mass against the missing transverse momentum component $\Delta p_{\perp}(y)$ (see text) for

a) events fitting the reaction $\pi^- p \to \pi^- \pi^+ \pi^- p$, and

b) non-fitting events.

Fig. 2 The cross section for the reaction $\pi^- p \to \pi^- \pi^+ \pi^- p$ as a function of laboratory momentum.

Fig. 3 The effective mass $M(\pi^- \pi^+ \pi^-)$ against $M(p\pi^+ \pi^-)$ for $\pi^- p \to \pi^- \pi^+ \pi^- p$ events. For $M(p\pi^+ \pi^-)$, the slower of the two π^-'s is taken.

Fig. 4 Effective mass distributions for a) $M(p\pi^+ \pi^-)$ and b) $M(\pi^- \pi^+ \pi^-)$ in the reaction $\pi^- p \to \pi^- \pi^+ \pi^- p$.

Fig. 5 Reaction mechanisms contribution to the channel $\pi^- p \to \pi^- \pi^+ \pi^- p$

Fig. 6 Relative rapidity (see text) of the slower π^- against that of the π^+ in the reaction $\pi^- p \to \pi^- \pi^+ \pi^- p$. The dotted lines correspond to "largest repidity gap" cuts.

FIG. 1

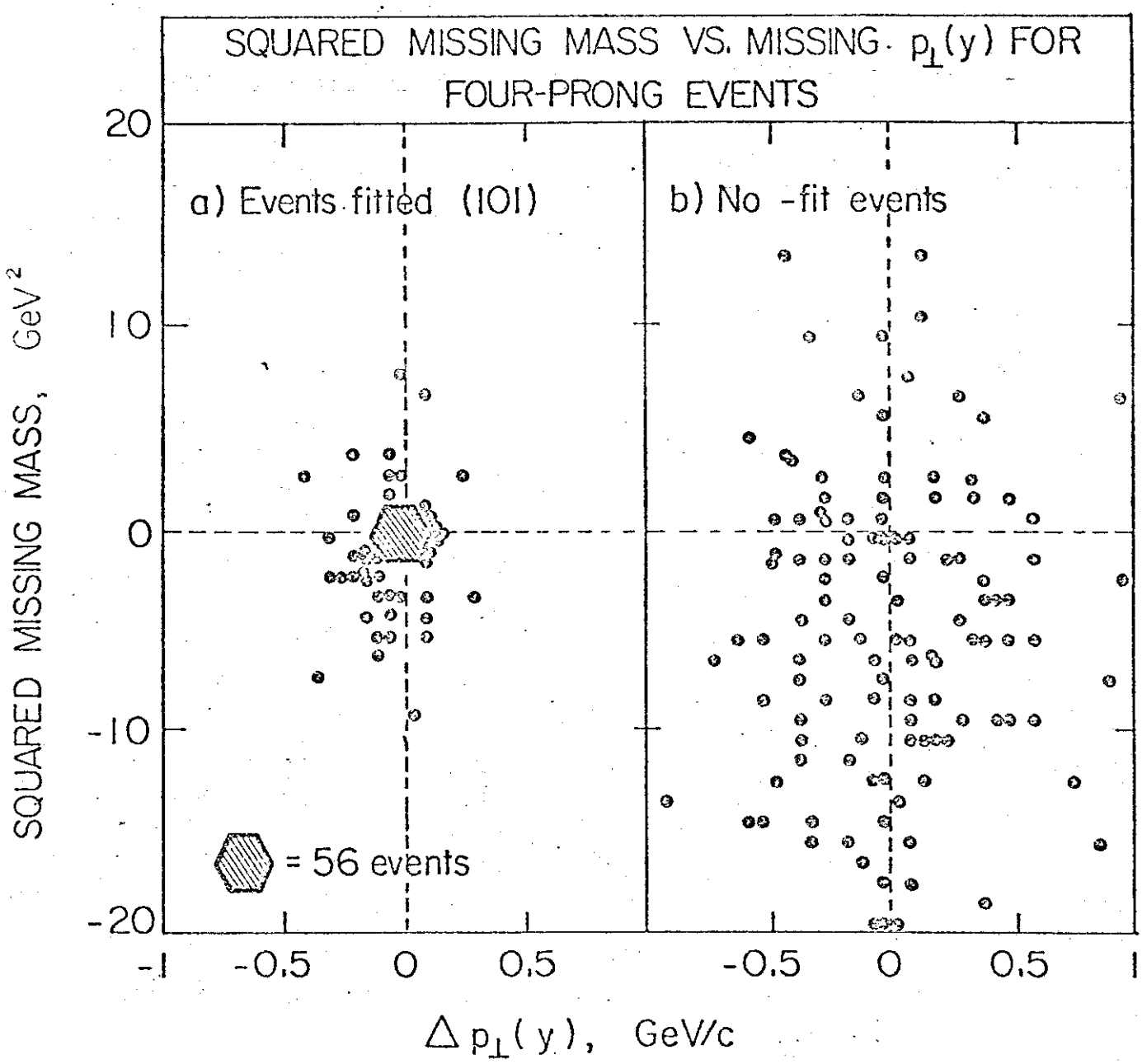
SQUARED MISSING MASS VS. MISSING $p_\perp(y)$ FOR FOUR-PRONG EVENTS
a) Events fitted (101)
b) No -fit events
= 56 events
SQUARED MISSING MASS, GeV^2
20
10
0
-10
-20
-1
-0.5
0
0.5
-0.5
0
0.5
1
$\Delta p_\perp(y)$, GeV/c

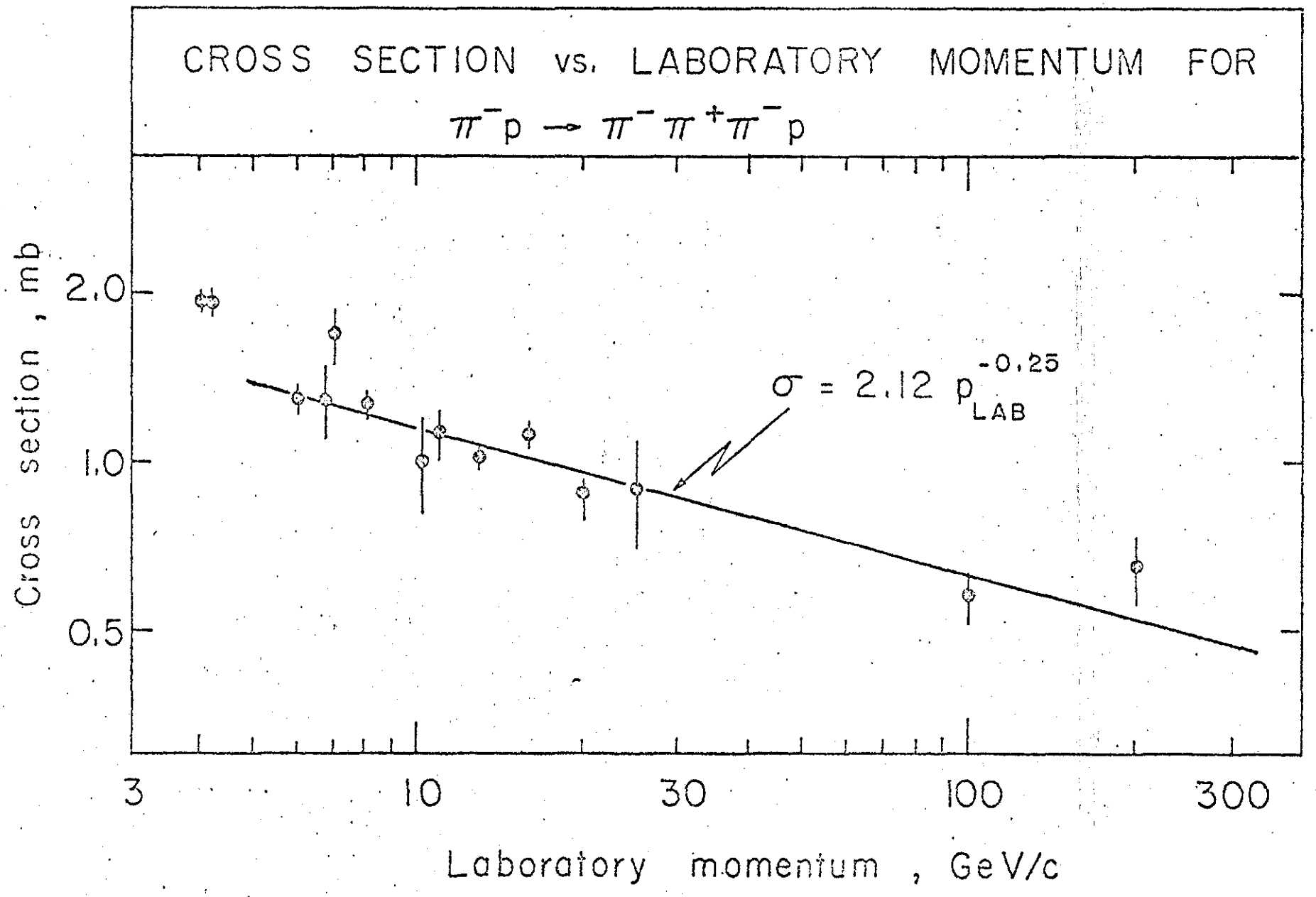
CROSS SECTION vs. LABORATORY MOMENTUM FOR
$\pi^- p \rightarrow \pi^- \pi^+ \pi^- p$
$\sigma = 2.12\ p_{LAB}^{-0.25}$
Cross section , mb
2.0
1.0
0.5
3
10
30
100
300
Laboratory momentum , GeV/c

FIG. 3

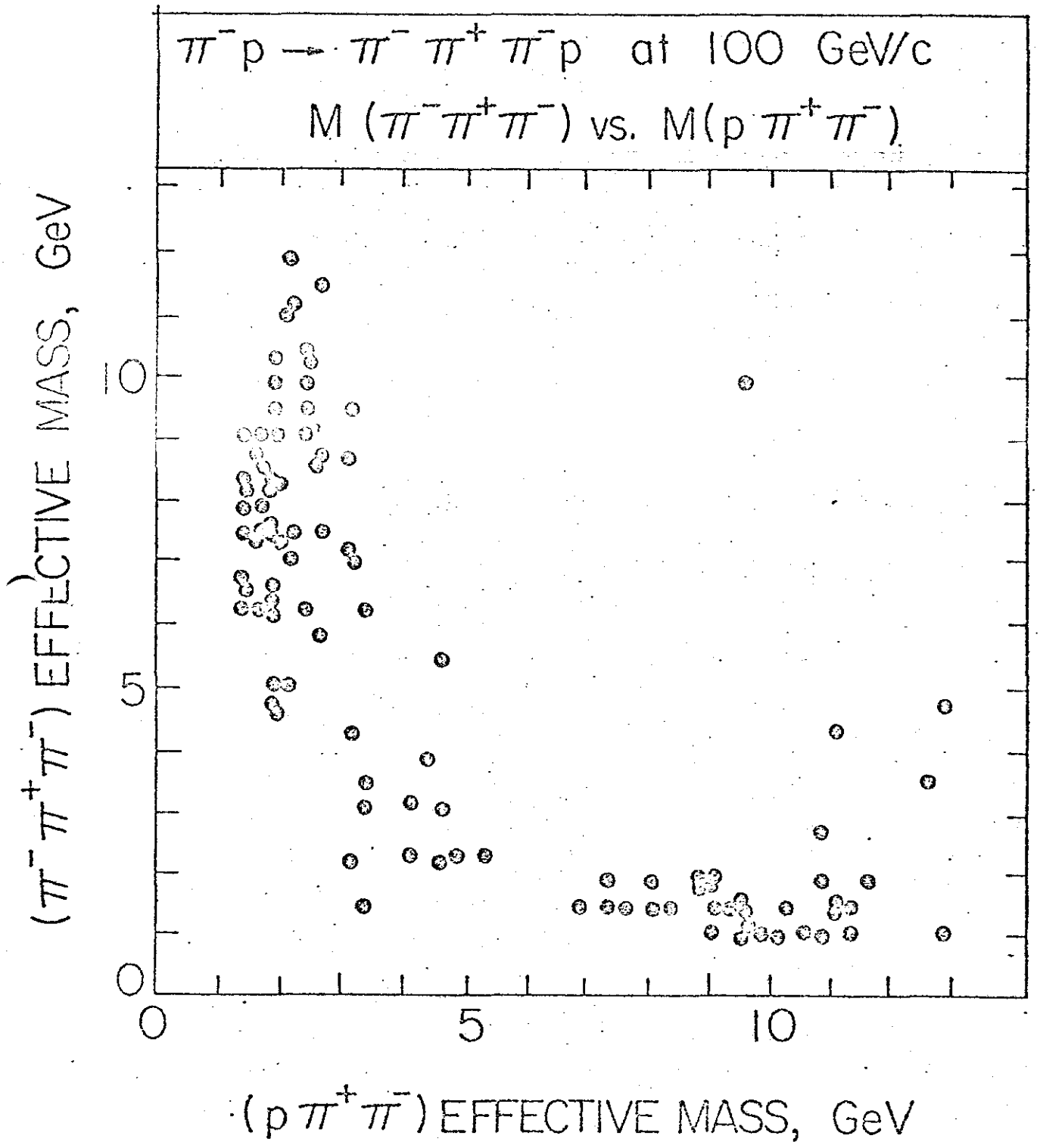
$\pi^- p \rightarrow \pi^- \pi^+ \pi^- p$ at 100 GeV/c
M ($\pi^- \pi^+ \pi^-$) vs. M($p \pi^+ \pi^-$)
($\pi^- \pi^+ \pi^-$) EFFECTIVE MASS, GeV
($p \pi^+ \pi^-$) EFFECTIVE MASS, GeV
0
5
10

FIG.4

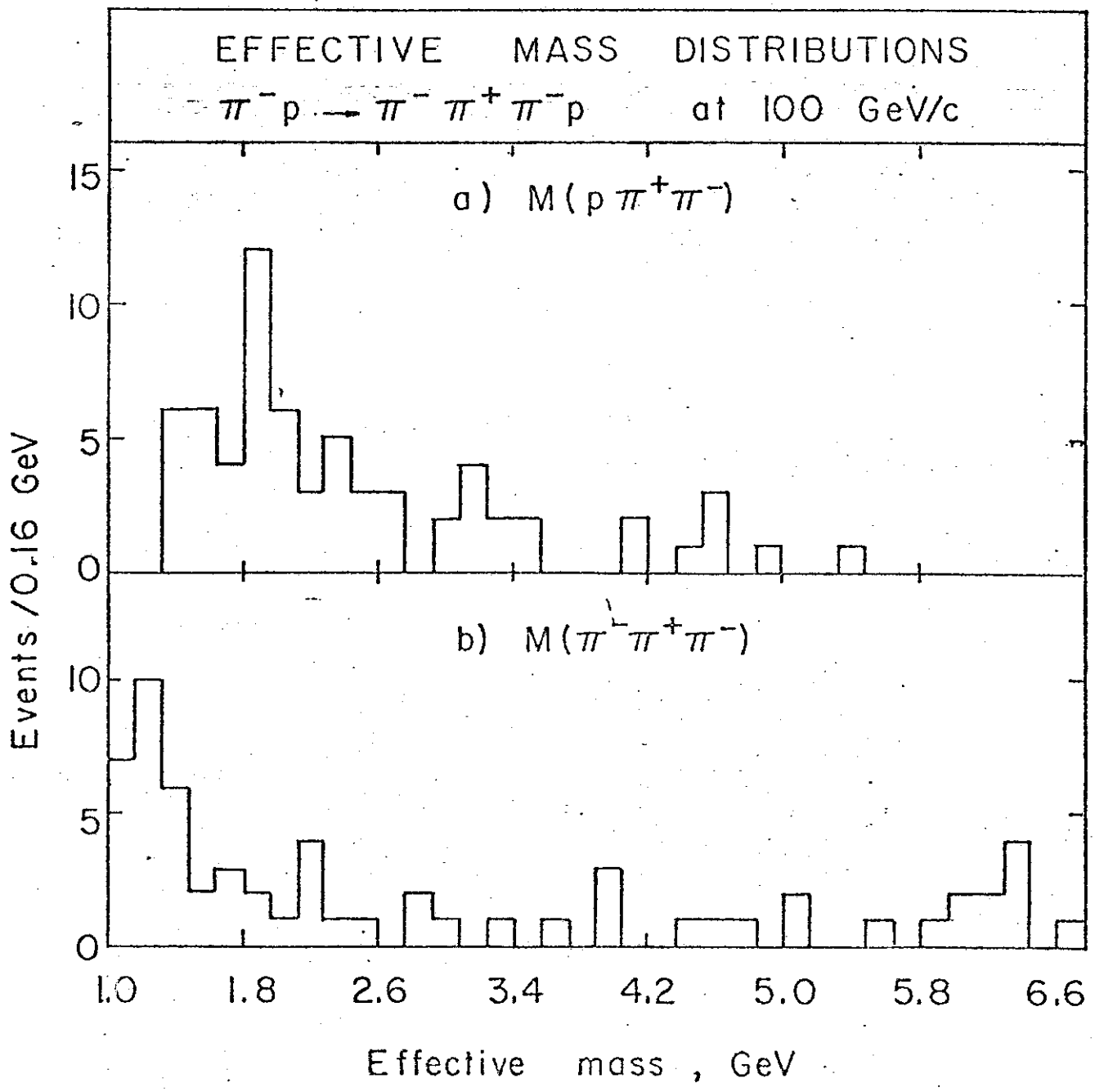
EFFECTIVE MASS DISTRIBUTIONS
$\pi^- p \rightarrow \pi^- \pi^+ \pi^- p$ at 100 GeV/c
a) $M(p\pi^+\pi^-)$
b) $M(\pi^-\pi^+\pi^-)$
Events /0.16 GeV
15
10
5
0
10
5
0
1.0
1.8
2.6
3.4
4.2
5.0
5.8
6.6
Effective mass , GeV

FIG 5

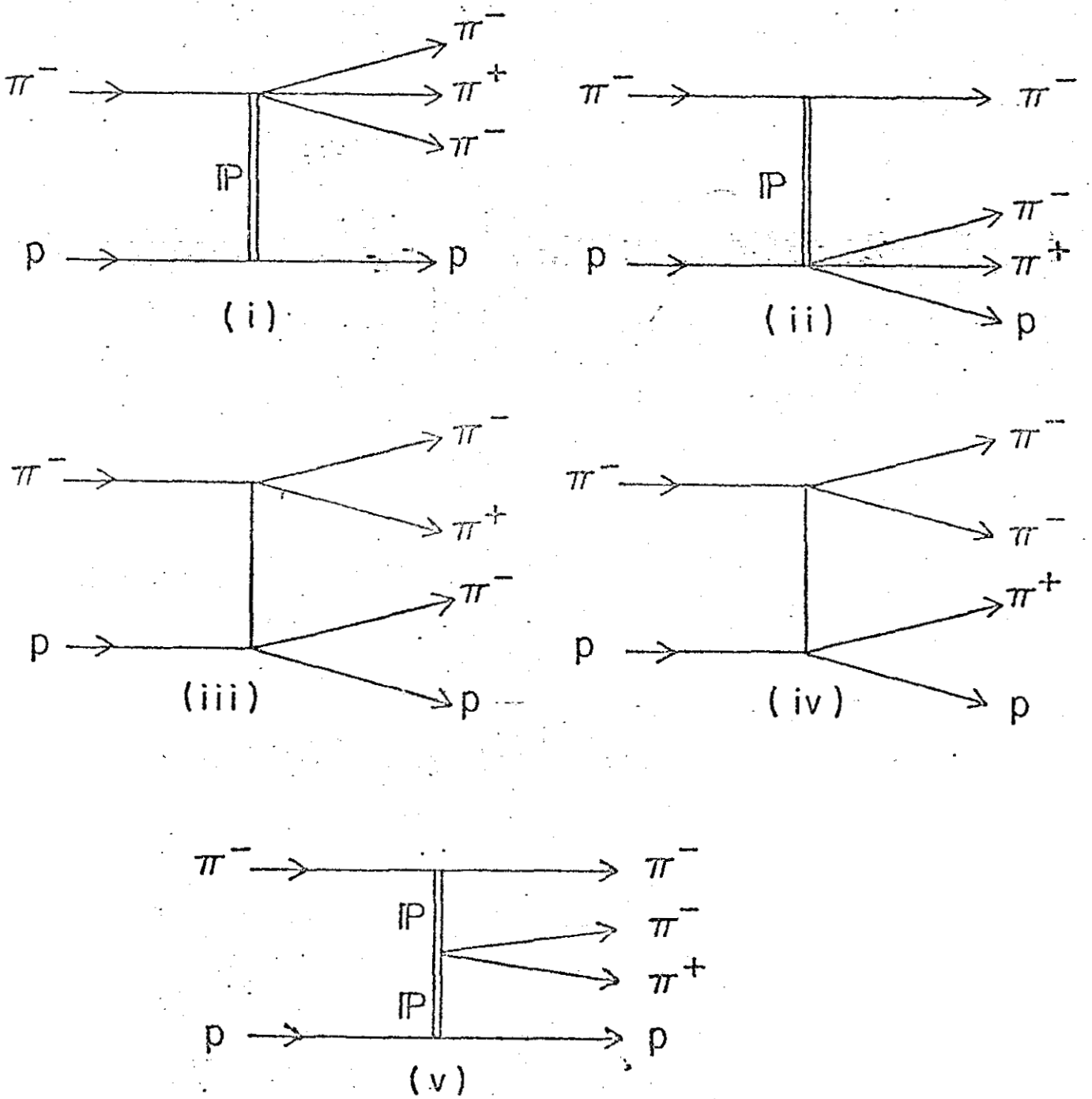

FIG. 6

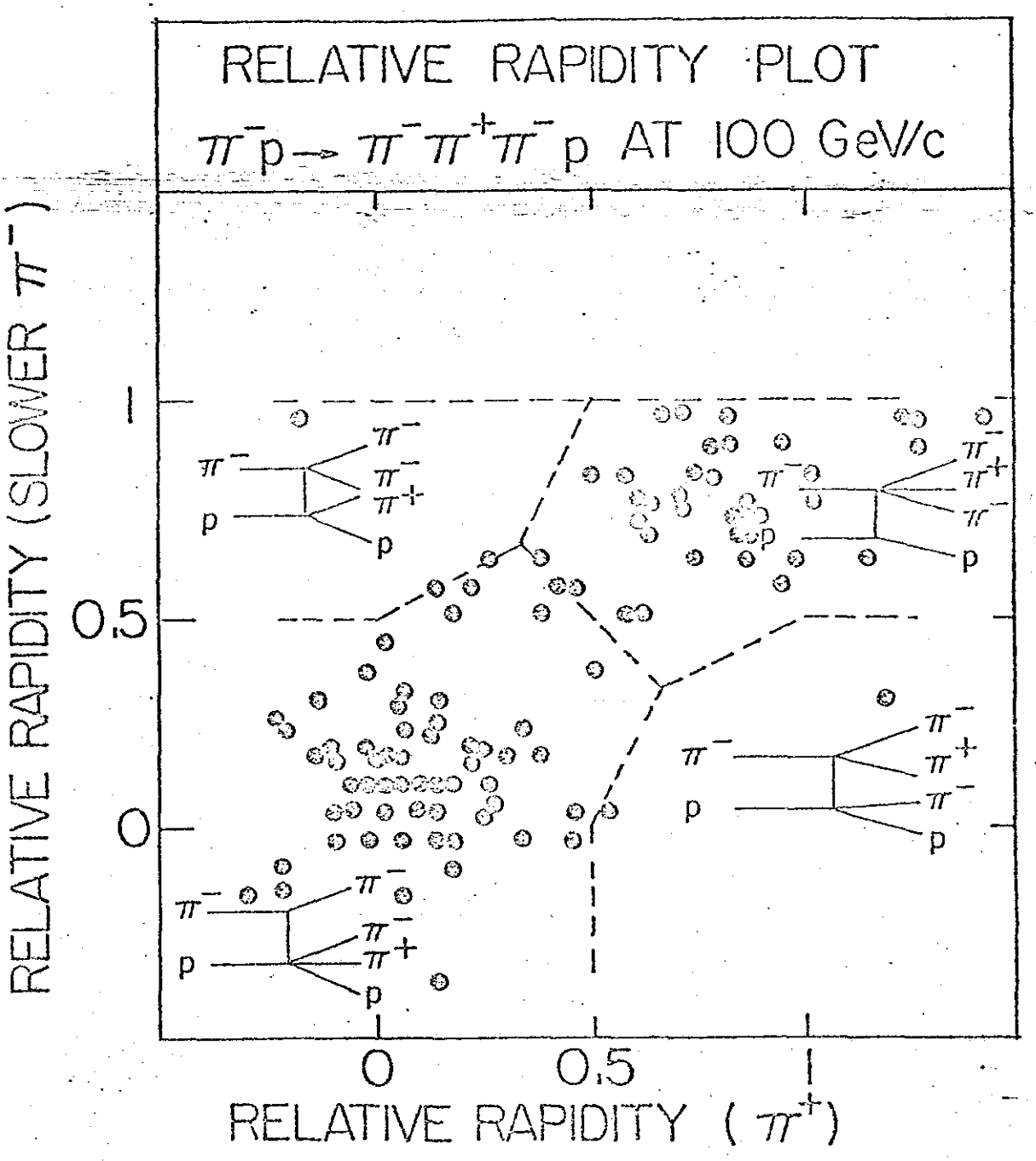
RELATIVE RAPIDITY PLOT
$\pi^- p \rightarrow \pi^- \pi^+ \pi^- p$ AT 100 GeV/c
RELATIVE RAPIDITY (SLOWER π^-)
RELATIVE RAPIDITY (π^+)
0
0.5
1
π^-
π^+
p